15TH IEA HEAT PUMP CONFERENCE
MAY 26–29, 2026 | HOFBURG
VIENNA 2026
DECARBONISATION THROUGH INNOVATION

Field Testing and Long-Term Numerical Evaluation of Horizontal Ground Heat Exchangers Installed via HDD Method at Saga Airport, Japan

Yuri Fushiki[a*], Hikari Fujii[a], Retsu Harada[b], Hiroyuki Kosukegawa[a], Saied Mohammadzadeh Bina[a], Takahiro Ogawa[a]

[a]Akita University, 1-1 Tegatagakuen-machi, Akita, 010-8502, Japan
[b]Biotex Inc. 1853-3 Tokuman, Kubota-cho, 849-0201, Saga, Japan

Abstract

This study investigates the long-term thermal performance of horizontally installed ground heat exchangers (GHEs) using horizontal directional drilling (HDD) at Saga Airport, western Japan, to improve the feasibility and cost-effectiveness of ground source heat pump (GSHP) systems. Building on field data from thermal response tests (TRTs), a numerical model of ground thermal behavior was developed using FEFLOW version 8.1 and was validated against measured temperatures, demonstrating its reliability for predictive long-term analysis. The validated model was then applied to five-year simulations of two GHE configurations (single-pass and double U-tube) and two layout arrangements (linear 1×20 and block 4×5) to assess thermal interference, heat extraction capacity, and subsurface thermal storage under realistic site conditions. The double U-tube configuration achieved slightly higher heat extraction rates than the single-pass configuration due to its larger heat transfer area; however, the coefficient of performance (COP) of the double U-tube was marginally lower, likely because of thermal interactions among adjacent U-tubes. The linear layout consistently outperformed the block-type layout, which exhibited more pronounced ground temperature rise and thermal accumulation. These results indicate that, under the studied conditions, thermal interference between GHEs has a stronger impact on system performance than subsurface thermal storage. The moderate performance difference between configurations suggests that simpler single-pass designs remain practical when installation cost and construction simplicity are prioritized. Overall, the results indicate that thermal interference between GHEs exerts a stronger influence on long-term performance than subsurface thermal storage. The study provides design-oriented insights for optimizing pipe configuration, spacing, and layout, and demonstrates the technical viability of HDD-installed horizontal GHEs as a practical option for shallow geothermal applications in cost-sensitive settings.

Keywords: Ground source heat pump; Horizontal ground heat exchanger; Horizontal directional drilling; FEFLOW; Thermal response test; Long-term simulation

1. Introduction

The widespread adoption of ground source heat pump (GSHP) systems has been constrained by the high installation cost of ground heat exchangers (GHEs), particularly under geologically complex subsurface conditions. While vertical GHEs are commonly employed due to their relatively small land footprint, they are often associated with elevated drilling costs and drilling challenges due to heterogeneous subsurface formations. In contrast, horizontal GHEs are generally more economical to install; however, they require a larger surface area, which can limit their applicability in urban or infrastructure-dense environments.

HDD has recently attracted attention as a viable trenchless method for the installation of horizontal GHEs. This technique allows for flexible and minimally invasive installation at various depths and orientations, offering a promising alternative for the deployment of GHEs beneath existing structures, roadways, or agricultural land. In Japan, several public-sector initiatives—such as those implemented in Saga Prefecture—have incorporated GSHP systems using HDD-installed GHEs as a part of broader regional strategies to achieve carbon neutrality. In particular, at Saga International Airport, horizontal GHEs were experimentally installed using the HDD method.

Previous studies have contributed to the conceptual development and empirical evaluation of HDD-based GHEs. For instance, Patino-Ramirez et al. (2020) proposed low-cost and low-risk design approaches of HDD, while Guo et al. (2020) conducted experimental evaluations on HDD drilling performance. Fujii et al. (2013) developed and validated numerical modeling approaches for slinky-type horizontal GHEs installed in shallow trenches, providing insights into the thermal behavior of conventionally buried horizontal systems. Additional work on underground thermal systems has further demonstrated the potential of subsurface heat utilization in built environments.

Previous numerical and experimental studies on horizontally installed ground heat exchangers have primarily focused on systems installed in shallow trenches, including linear-loop, spiral-coil, and slinky-type configurations. For example, Dasare and Saha (2015) numerically investigated the thermal performance of horizontal GHEs under high energy demand conditions, highlighting the influence of ground properties and operating parameters. Hu et al. (2023) compared the thermal behavior of linear-loop, spiral-coil, and slinky-coil horizontal GHEs, demonstrating that exchanger geometry plays a critical role in heat transfer efficiency. In addition, Luo and Gan (2024) examined thermal interference effects in slinky-type horizontal GHEs, emphasizing the importance of spacing and layout in system performance. While these studies provide valuable insights into the thermal characteristics of horizontal GHEs, their findings are primarily derived from trench-installed systems and may not fully represent the installation geometry and boundary conditions associated with HDD-installed horizontal GHEs.

To address this limitation, a collaborative research initiative was launched in 2018 by the Energy Resource Engineering Laboratory at Akita University in partnership with Biotex Co., Ltd. As part of this initiative, a comparative study was conducted in 2020 to evaluate the heat exchange performance of vertical and HDD-installed horizontal ground heat exchangers installed at the same field site. The results showed that, although the vertical ground heat exchangers exhibited marginally higher heat exchange performance, the difference was not substantial. Furthermore, the horizontal configuration was found to be more favorable from a cost perspective when installing a larger number of heat exchangers.

Building on these findings, the present study focuses on the performance evaluation and numerical modeling of HDD-installed horizontal GHEs, with particular emphasis on the performance differences between single-pass and double U-tube configurations using a field-calibrated numerical model. As a part of planned GSHP system deployment at Saga International Airport, TRTs were conducted as a preliminary investigation. These data provide a basis for validation of numerical simulations for system design.

The present study aims to simulate the long-term performance of horizontal GHEs under actual field conditions by refining the previously developed and validated numerical model based on TRT data. Specifically, the simulation compares the heat exchange performance between single-pass and double U-tube configurations over a five-year period. In addition, the effects of different GHE layouts, including variations in GHE configuration and spacing, were examined to evaluate their influence on thermal performance and short-term thermal interaction under site-specific operating conditions.

Figure 1. HDD drilling operation during the installation of horizontal GHEs

2. Methods/Approach

2.1. Site Conditions and Field Measurements

2.1.1. Site description and GHE installation

In this study, one vertical and six horizontal GHEs were installed near the airport parking area at Kyushu Saga International Airport, located in western Japan, as a pilot installation (Figure 2 (a), (b)). The subsurface consists of alternating layers of sand and gravel (Figure 2 (c)), with groundwater level located at a depth of approximately 5 meters. The ground surface is paved with asphalt. Saga Prefecture has a relatively mild climate compared to other regions in Japan, resulting in a greater demand for cooling than for heating. These GHEs are expected to contribute to future geothermal system designs for airport Heating, Ventilation, and Air Conditioning (HVAC) applications.

This study primarily focused on the horizontal GHEs. The TRTs were conducted on all the six horizontal GHEs, including four single-pass, one single U-tube, and one double U-tube configuration (Figure 3 (a), (b), (c)). In the single-pass configuration, the borehole diameter was 115 mm, and the pipe had inner and outer diameters of 50 mm and 63 mm. In contrast, for both the single U-tube and double U-tube configurations, the borehole diameter was 165 mm, and the pipes had inner and outer diameters of 25 mm and 32 mm. The well path of the double U-tube is shown as a representative example in Figure 3(d). Other horizontal GHEs were installed with similar well paths at a burial depth of approximately 5 m.

For the single-pass configurations, TRTs were conducted to assess thermal interference between horizontal GHEs. During the experiments, heated water was circulated through a horizontal single-pass arrangement with a total length of roughly 200 m, at a heat exchange rate of 20 W/m of pipe. The effect of thermal interference on the temperature rise of the heat carrier fluid was evaluated by varying the spacing between the supply and return pipes at 1 m, 2 m, and 4 m (Figure 3 (e)). The results indicated that thermal interference was observed by the seventh day of circulation in the 1 m spacing configuration, while it was slightly observed on the 27th day for the 2 m spacing. No thermal interference was detected in the 4 m spacing configuration over the 20-day testing period. These findings confirm that increasing the pipe spacing reduces thermal interference, and that 2 m spacing provides a practical balance between mitigating interference and minimizing the required installation area (Ogawa et al., 2026).

For the single U-tube and double U-tube configurations, TRTs were conducted to estimate the soil thermal conductivity using the semi-logarithmic interpretation and to compare their respective heat exchange capacities. The results indicated that the thermal conductivity of the subsurface was approximately 1.0 W/m/K. This relatively low value is likely attributable to the predominance of clay-rich sediments at the site, and it also suggests minimal groundwater flow within the depth range of the GHEs. Furthermore, the double U-tube exhibited higher heat exchange performance than the single U-tube (Fushiki et al., 2025).

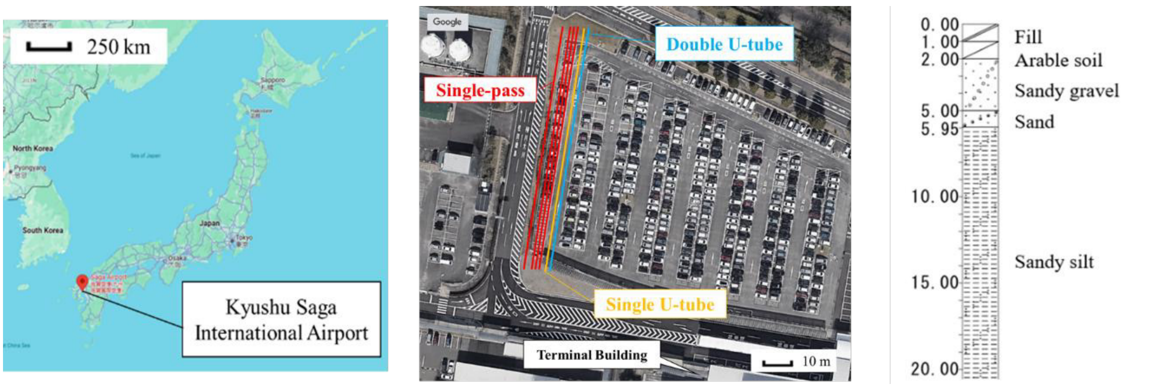

(a) Site location (b) GHEs arrangement (c) Geological column

Figure 2. Site overview and geological information.

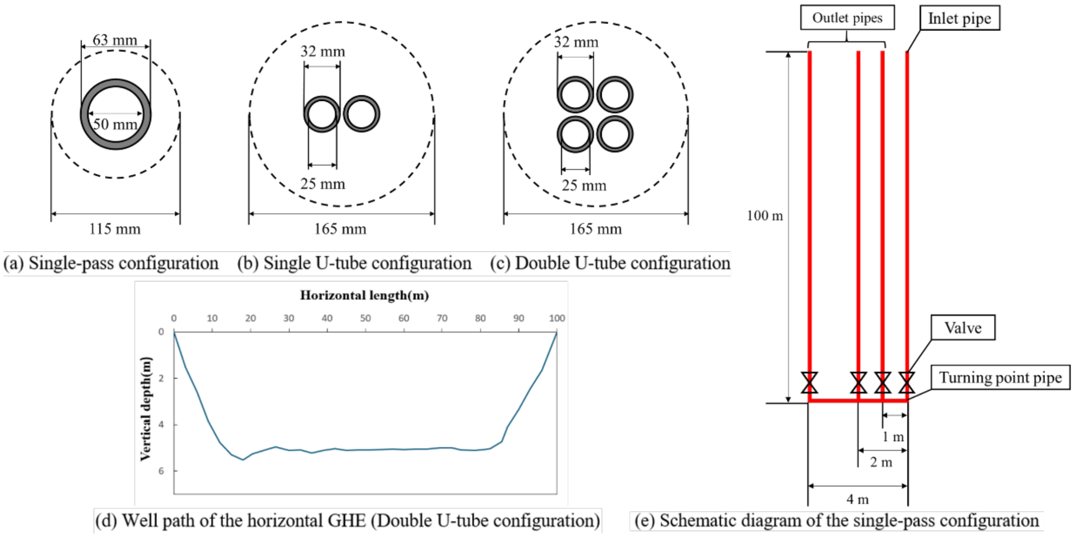

Figure 3. Cross-sectional views of GHEs and GHE information

2.1.2. TRT Results

Among multiple TRTs performed at the site, the test result of the horizontal double U-tube system was selected for analysis in this study, in order to reproduce the thermal characteristics of the ground at this field site. The TRT was conducted from November 16 to 21, 2024. Heated water was circulated at an average flow rate of 19.8 L/min with an average heat load of 42.0 W/m for two days. The circulation and heating were then stopped, and the temperature recovery of the ground was monitored for three days using a fiber-optic temperature sensor installed in one of the inlet pipes of a double U-tube.

Figure 4 (a) presents the inlet and outlet temperatures of the heat medium, the flow rate, and the heat load recorded during the heating test period. These parameters were measured stably throughout the test, confirming that the TRT was conducted under appropriate conditions. Figure 4 (b) illustrates the recovery of ground temperatures, showing that it gradually returned to its initial condition over time following the termination of the circulation. The recovery was observed consistently throughout the site, indicating the absence of locations with locally elevated thermal conductivity.

As shown in Figure 5, the average thermal conductivity of the ground was estimated using a graphical method based on the linear portion of the temperature rise curve, yielding a value of 1.09 W/m/K. The thermal conductivity was evaluated using the infinite line-source (ILS) model, which is widely applied in the interpretation of thermal response tests. According to the ILS theory, the increase in fluid temperature exhibits a linear relationship with the logarithm of time, and the slope of this relationship is inversely proportional to the ground thermal conductivity. The thermal conductivity was determined from the slope of the temperature versus ln(time) curve following the formulation proposed by Ingersoll and Plass (1948). The relatively low thermal conductivity is likely due to the predominance of clay-rich sediments at the site, which also suggests that groundwater flow had an insignificant influence under these conditions.

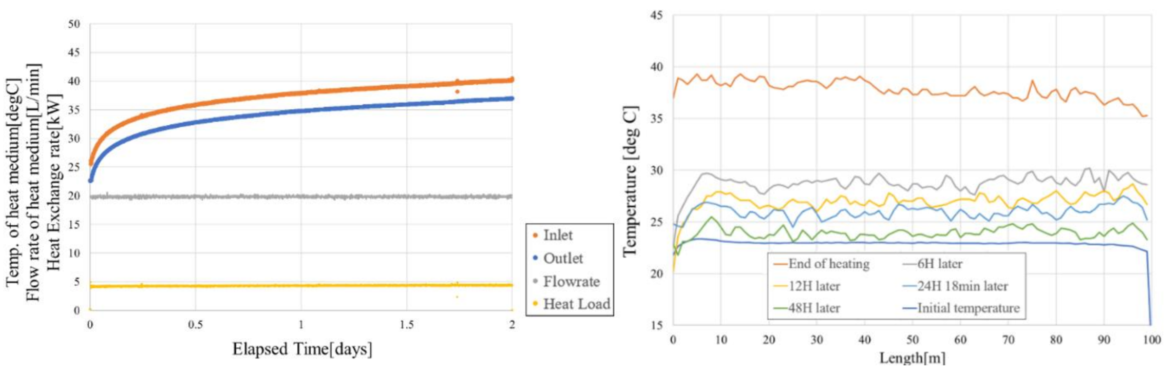

(a) Measurements during the TRT heating period

(b) Ground temperature during the recovery period

Figure 4. Measured Values of TRT (a) Measurements during the TRT heating period: heat medium temperatures, circulation flow rate, and heat load (b) Ground temperature measurements during the recovery period

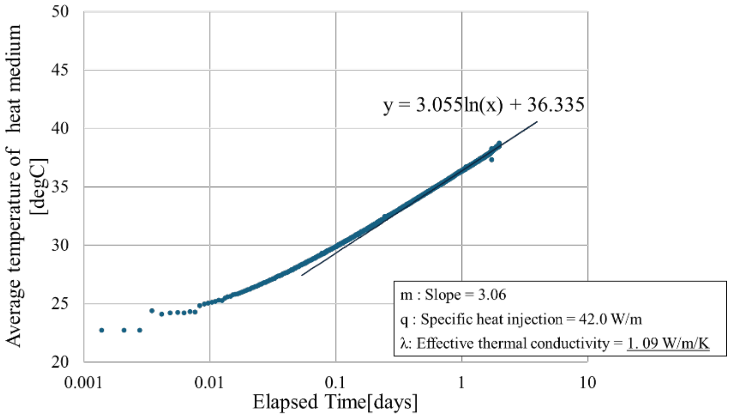

Figure 5. Average ground thermal conductivity estimated from the temperature rise curve

2.2. Model Development and History Matching

The TRT results, including the estimated ground thermal conductivity and the observed temperature recovery, were used to inform the development of a numerical model of the horizontal double U-tube GHE system. The model was constructed using FEFLOW version 8.1, with a domain extending 120 m, 20 m, and 26 m in the x, y, and z directions, respectively (Figure 6). The shallow zone of the ground is affected by surface air temperature (SAT), and therefore a finer mesh was applied near the ground surface. AT, an equivalent outdoor temperature accounting for air temperature, solar radiation, and surface properties, is defined as Equation (1):

$$SAT = \theta_0 + \frac{1}{\alpha_0}\left((1-\alpha_s)\,J - \varepsilon\, J_{eh}\right) \tag{1}$$

where SAT denotes the soil–air temperature [°C]; θ_0 is the ambient air temperature [°C]; α_0 represents the overall heat transfer coefficient between air and soil [W/m²·K] α_s is the albedo; J is the total solar radiation [W/m²]; ε is the longwave emissivity [dimensionless]; and J_{eh} is the effective emission [W/m²]. An albedo of 0.12 was assumed for asphalt surfaces.

As initial conditions, the subsurface temperature was uniformly set to 20.0°C, which is reasonable considering that the annual mean air temperature in Saga City in 2024 was 18.8°C and that undisturbed subsurface temperatures are typically 1–2°C higher than the annual mean. The thermal conductivity of the subsurface was set to 1.0 W/m/K based on the TRT results. An effective thermal conductivity accounting for both soil and water was used, and groundwater flow was not considered, simplifying the model. The volumetric heat capacity was set to 2.19×10^6 J/m³·K. During the simulation, the upper boundary of the model was assigned the SAT calculated from the published data of the Saga Local Meteorological Observatory, while the lower boundary was fixed at a constant temperature of 20 °C. The lateral boundaries were placed sufficiently far from the GHE and were treated as adiabatic (no heat flux).

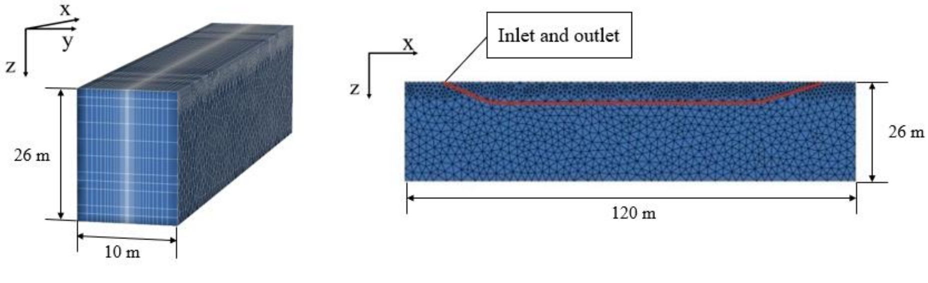

Figure 6. Two-dimensional (x–z plane) and three-dimensional views of the numerical models

The validity of the developed numerical model for the horizontal GHE was verified by comparing the measured data obtained from the TRT with the simulated outlet fluid temperature and ground temperature during the recovery period. Figure 7 presents a comparison of the measured and simulated outlet fluid temperatures. At the end of the heating period, the measured outlet temperature was 32.5 °C, and the simulated value was 32.2 °C, resulting in a difference of 0.3 °C. The measured and simulated outlet temperatures of the heat carrier are in good agreement throughout the heating period, indicating that the model accurately reproduces the temperature response of the system. Figure 8 presents the comparison of measured and simulated ground temperature profiles at the end of the heating period and 6, 12, and 48 h after the end of heating. Although fluctuations in ground temperature are observed during the early stage of the recovery period, the simulated and measured temperatures show good agreement through the recovery period, indicating high reproducibility. These results confirm that the numerical model appropriately reproduces the thermal behavior observed experimentally.

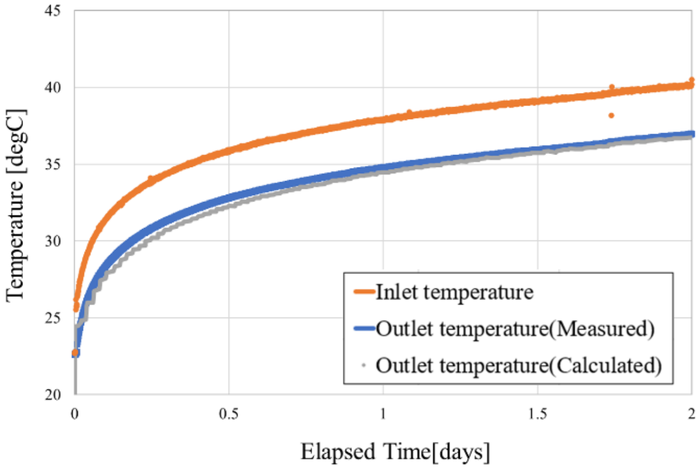

Figure 7. Comparison between simulated and measured outlet temperatures

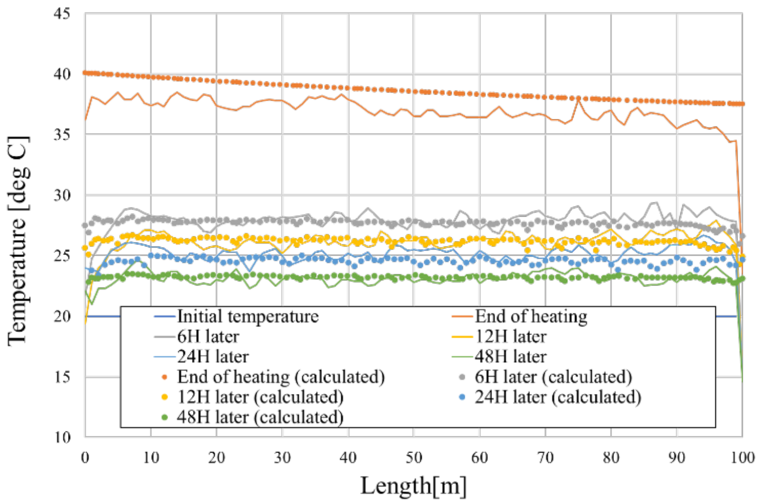

Figure 8. Comparison between simulated and measured ground temperatures

2.3. Case Study: Long-Term Simulation

2.3.1. Simulation Conditions

Assuming a five-year operation period, a one-year cycle consisting of four months of heating, a two-month non-operating period, four months of cooling, and another two-month non-operating period was assumed. The heat exchange rate at which the GHE outlet temperature reaches 35 °C during the cooling operation in summer was then calculated. The threshold of 35°C was set under the assumption that beyond this temperature, the ground loses its advantage as a heat sink compared to an air-source system. A higher heat exchange rate at the time the outlet temperature reaches 35°C indicates more efficient heat exchange with the ground.

The conditions for the case study are summarized in Table 1. In this study, the input parameter was the heat load, and simulations were conducted at 50, 60, and 70 kW to identify the heat exchange rates at which the GHE outlet temperature exceeds 35 °C during summer cooling. Of the total 1,250 kW thermal load required for heating and cooling an airport terminal building, it is assumed that 500 kW is provided by GSHP as a base load. Based on this assumption, the required heat exchange rates are 600 kW for cooling and 375 kW for heating. These values were derived using the assumed coefficients of performance (COP) of 5.0 for cooling and 4.0 for heating. Assuming a heat extraction rate of 30 W/m for each GHE, a total GHE length of 20,000 meters would be required to meet these loads. Given that each GHE is 100 meters long, this corresponds to 200 boreholes. For this case study, 20 of these GHEs were selected for detailed analysis.

Table 1. Simulation Conditions

Duration (year)	One-year cycle		Operation time per day (hours/day)	Heat exchange rate (kW)		Flow rate (L/min)
	Cooling and heating period	Outage period		Cooling	Heating	
5	4 months each	2 months each	12	60	37.5	20

2.3.2. Numerical Models for the Case Study

In this case study, the numerical model developed in Section 2.2 was further modified to simulate a long-term operation scenario. Specifically, a system comprising 20 GHEs was modeled, and a five-year simulation was conducted to evaluate its potential application for future heating and cooling of the airport terminal building. Two numerical models were developed to evaluate the performance of different GHE configurations, assuming both single-pass and double U-tube systems. In the first model titled "1×20 model", 20 GHEs were installed in a straight line at a depth of 6 meters, arranged horizontally and parallel to the ground surface (Figure 9 (a)). In the second model referred to as the "4×5 model", the GHEs were arranged in a block-like shape, with five GHEs placed in each of four vertical layers (4 m, 6 m, 8 m, and 10 m), forming a compact cluster in a cross-sectional view (Figure 9 (b)). In both simulation models, the lateral and bottom boundaries were located 20 meters away from the GHEs to minimize boundary effects. The numerical domain was subdivided into 140 layers along the y–z plane, with each layer 1 meter thick, allowing precise capture of vertical temperature variations. A spacing of 2 meters between adjacent GHEs was applied, following the recommendations of Ogawa et al., 2026, which minimizes thermal interference while maintaining feasible construction conditions. The subsurface thermal properties and initial temperature were based on the history-matched model in Section 2.2, with a thermal conductivity of 1.0 W/m/K and an initial temperature of 20 °C. SAT variations were applied at the ground surface to account for seasonal changes. Based on the settings described above, long-term simulations were performed for both the single-pass and double-U-tube configurations, and the results were compared to evaluate their relative performance.

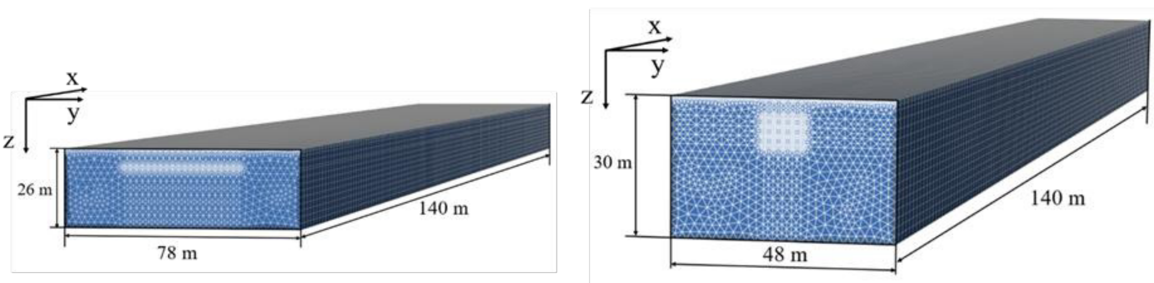

(a) 1×20 model (b) 4×5 model

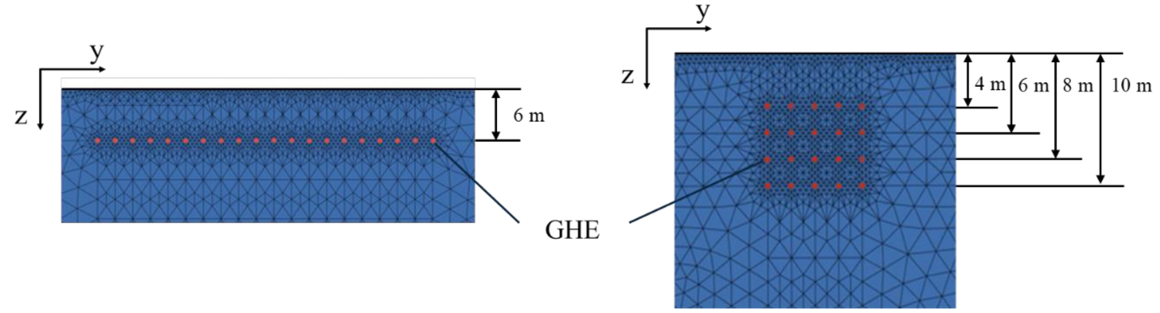

(c) 1×20 model (d) 4×5 model

Figure 9. Three-dimensional views of (a) the linear arrangement and (b) the block-type arrangement, and two-dimensional close-up views around the borehole (y–z plane) for (c) the linear arrangement and (d) the block-type arrangement.

3. Results and Discussion

The numerical model was run for a five-year simulation, which included both cooling and heating operations. During the cooling operation, if the outlet temperature exceeds 35 °C, the GHE was considered insufficient compared to the ambient air temperature. Therefore, the maximum allowable heat extraction rates were determined to ensure that the outlet temperature does not exceed 35 °C over a five-year period. According to Figure 10 (a), in the single-pass configuration with the 1×20 model, the outlet temperature remained below 35 °C at a heat extraction rate of 60 kW but exceeded 35 °C at 70 kW. In contrast, Figure 10 (b) shows that in the 4×5 model, the outlet temperature stayed below 35 °C at 50 kW but exceeded it at 60 kW. These results suggest that the 1×20 model can accommodate higher thermal loads than the 4×5 model. At 60 kW, the 4×5 configuration exhibited higher final outlet temperatures, suggesting heat accumulation. Moreover, outlet temperatures in the 4×5 configuration increased more rapidly over the five-year period, likely due to greater thermal interference between adjacent pipes.

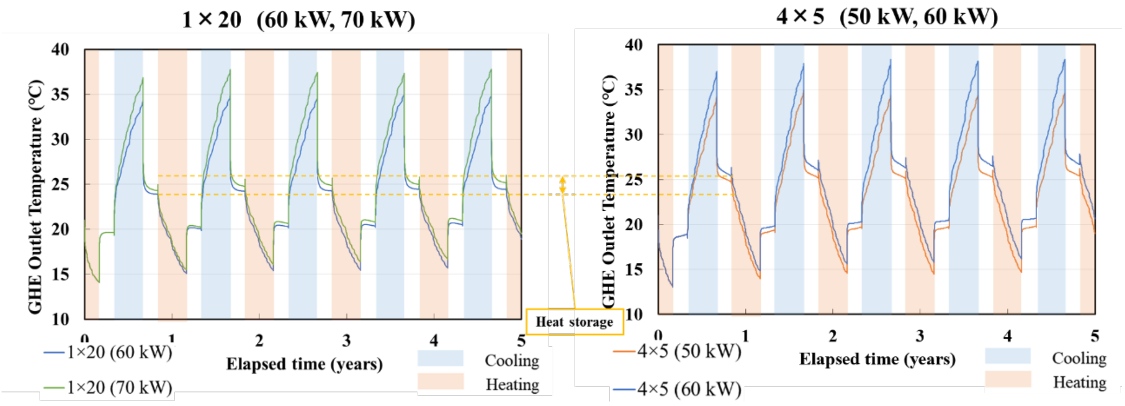

(a) 1×20 model (b) 4×5 model

Figure 10. 5-year simulation of the single-pass configuration

Similarly, for the double U-tube configuration, as shown in Figure 11 (a), the outlet temperature in the 1×20 model remained below 35 °C at 60 kW but exceeded it at 70 kW. In the 4×5 model (Figure 11 (b)), the outlet temperature did not exceed 35 °C at 50 kW but exceeded it at 60 kW. The 1×20 model tolerated higher heat extraction rates than the 4×5 model. At 60 kW, the 4×5 model showed higher final outlet temperatures than the 1×20 model, indicating heat accumulation. The more rapid temperature increases in the 4×5 model may be attributed to increased thermal interference, consistent with the single-pass case.

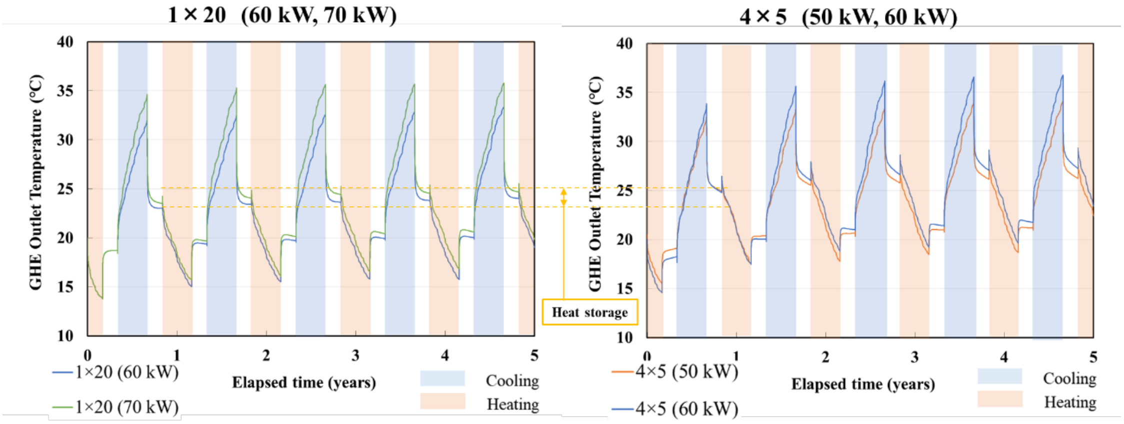

(a) 1×20 model

(b) 4×5 model

Figure 11. 5-year simulation of the double U-tube configuration

Table 2 summarizes the simulation results regarding the heat extraction rates at which the outlet temperature reached 35 °C after five years of cooling operation, for both the single pass and double U-tube configurations. According to Table 2, the maximum allowable heat exchange rate during cooling operation was 60.6 kW for the single-pass configuration and 62.6 kW for the double U-tube configuration in the 1×20 model. In the 4×5 model, the corresponding values were 51.0 kW and 52.9 kW, respectively. A comparison of Tables 2(a) and 2(b) indicates that the double U-tube achieved slightly higher maximum allowable heat exchange rates than the single-pass configuration in both models. Since the difference in heat exchange rates is relatively small, the additional cost associated with the more complex pipe arrangement should be considered when assessing installation expenses.

Furthermore, when comparing the 1×20 and 4×5 models, both configurations exhibited higher heat exchange rates in the 1×20 model. This can be attributed to the smaller GHE density in the 1×20 layout, which mitigates thermal interference among boreholes. As illustrated in Figures 10 and 11, although heat accumulation was observed in the ground for the 4×5 model, heat accumulation did not enhance system performance during either summer or winter operation. These findings suggest that thermal interference among GHEs exerts more significant influence than heat accumulation, ultimately exerting a negative effect on overall system performance.

Table 2. Maximum allowable heat extraction rates at which the outlet temperature reached 35 °C after five years

(a) Single-pass configuration

Model	Heat Exchange Rate				Flow Rate
	Cooling		Heating		
	kW	W/m	kW	W/m	L/min
1×20	60.6	30.3	37.5	18.8	20.0
4×5	51.0	25.5			

(b) Double U-tube configuration

Model	Heat Exchange Rate				Flow Rate
	Cooling		Heating		
	kW	W/m	kW	W/m	L/min
1×20	62.6	31.3	37.5	18.8	20.0
4×5	52.9	26.5			

Then, for the 1×20 model, the COP of the heat pump was calculated for both the single-pass and double U-tube configurations under a heat exchange rate of 60 kW, based on the results of the five-year simulation (Table 3). The COP of the heat pump system was determined using the correlation equations (2) and (3), which were derived from the performance curves of the water-to-water heat pump GSHP-1001 manufactured by Sunpot Co., following the method of Fujii et al. (2014).

$$COP_{cooling} = -0.22T_{in} + 11.56 \quad (2)$$

$$COP_{heating} = 0.104T_{in} + 3.14 \quad (3)$$

Here, $COP_{cooling}$ represents the coefficient of performance during cooling, $COP_{heating}$ represents five-years average of coefficient of performance during heating, and T_{in} denotes the inlet temperature of the fluid entering the heat pump [°C]. According to Table 3 the single-pass configuration exhibited a COP of 5.07 during cooling operation and 5.13 during heating operation, while the double U-tube configuration showed a COP of 5.58 during cooling and 5.14 during heating. These results indicate that the COPs for heating are nearly identical between the two pipe configurations, whereas the COP during cooling is slightly higher for the double U-tube configuration. This can be attributed to the higher heat exchange rate set for cooling (30 W/m) compared to heating (18.8 W/m), which makes differences in COP more pronounced during cooling operation.

Table3. COPs of the single-pass and double U-tube configurations at 60 kW for the 1×20 model

	Cooling	Heating
Single-pass configuration	5.07	5.13
Double U-tube configuration	5.58	5.14

4. CONCLUSION

In this study, the long-term thermal performance of GHEs installed horizontally using the HDD method at Saga Airport in western Japan was investigated. The aim was to improve the feasibility of GSHP systems by evaluating the thermal performance and long-term operational characteristics of HDD-installed horizontal ground heat exchangers. First, among multiple TRTs conducted on horizontal GHEs at the site, the test data of the double U-tube system were analyzed. Using these data, a numerical model that reproduced the thermal characteristics of the ground was developed with FEFLOW version 8.1. The model was validated by showing good agreement between simulated and measured values. This validated model was then applied to perform long-term simulations. Two GHE configurations (single-pass and double U-tube) and two arrangement layouts (1×20 and 4×5) were analyzed to evaluate thermal interference, heat extraction capacity, and subsurface thermal accumulation. The double U-tube configuration exhibited slightly higher heat extraction rates than the single-pass configuration due to its larger heat transfer surface area. Furthermore, the 1×20 arrangement demonstrated higher heat exchange rates for both configurations compared with the 4×5 layout, which showed more pronounced temperature rise and heat accumulation within the ground. These results indicate that, under the studied conditions, thermal interference among GHEs, which causes localized increases in ground temperature, has more negative impact on overall system performance than the positive effects of subsurface heat accumulation. A comparison of COPs showed that heating performance was nearly identical between the two configurations. The performance difference between the single-pass and double U-tube designs was moderate, indicating that configuration type alone does not strongly influence overall system efficiency. Overall, both configuration type and layout implications are critical factors for achieving efficient and reliable long-term operation of horizontally installed GHEs.

References

[1] Patino-Ramirez F, Layhee C, Arson C. Horizontal directional drilling (HDD) alignment optimization using ant colony optimization. Tunnelling and Underground Space Technology. 2020;103:103450. https://doi.org/10.1016/j.tust.2020.103450

[2] Guo Z, Xie S, Ren L, Gong Y, Dong C. Pipeline lifting mechanics research of horizontal directional drilling. Mathematical Problems in Engineering. 2020;2020:5038532. https://doi.org/10.1155/2020/5038532

[3] Fujii H, Yamasaki S, Maehara T, Ishikami T, Chou N. Numerical simulation and sensitivity study of double-layer Slinky-coil horizontal ground heat exchangers. Geothermics. 2013;47:61–68.

[4] Bourne-Webb PJ, Burlon S, Javed S, Kürten S, Loveridge F. Analysis and design methods for energy geostructures. Renewable and Sustainable Energy Reviews. 2016;65:402–419. https://doi.org/10.1016/j.rser.2016.06.046

[5] Dasare, R. R., Saha, S. K. (2015). Numerical study of horizontal ground heat exchanger for high energy demand applications. Applied Thermal Engineering, 85, 252–263. https://doi.org/10.1016/j.applthermaleng.2015.04.014.

[6] Hu, L., Rizvi, Z.H., Tobber, L., Wuttke, F. (2023). Thermal performance of three horizontal ground heat exchanger systems: comparison of linear-loop, spiral-coil and slinky-coil arrangements. Frontiers in Energy Research, 11:1188506. https://doi.org/10.3389/fenrg.2023.1188506

[7] Luo, M., Gan, G. (2024). Numerical investigation into the thermal interference of slinky ground heat exchangers. Applied Thermal Engineering, 248(Part A), 123215.

[8] Fushiki Y, Fujii H, Harada R, Kosukegawa H, Mohammadzadeh S. Field test-based comparative analysis of heat exchange performance in vertical and horizontal ground heat exchangers for geothermal applications. In: Proceedings of the 50th Workshop on Geothermal Reservoir Engineering. SGP-TR-229; 2025.

[9] Ogawa T, Fujii H, Harada R, Kosukegawa H, Mohammadzadeh S. Evaluation of thermal interference between horizontal ground heat exchangers. In: Proceedings of the World Geothermal Congress 2026. (in print).

[10] Ingersoll, L.R., Plass, H.J., 1948. Theory of the ground pipe heat source for the heat pump. Heating, Piping and Air Conditioning 20, p. 119–122.

[11] Fujii H, Maehara T, Katsuragi M. Field test and numerical modeling of an aquifer thermal energy storage system. J Geotherm Res Soc Japan. 2014;36(3):109–120. (In Japan with English abstract)